Remote Sensing Applications: Society and Environment 14 (2019) 207–223

Contents lists available at ScienceDirect

Remote Sensing Applications: Society and Environment

journal homepage: www.elsevier.com/locate/rsase

Identifying and extracting a seasonal streamflow signal from remotely sensed snow cover in the Columbia River Basin

Benjamin Washington[a,*], Lynne Seymour[a], Thomas Mote[b], David Robinson[c], Thomas Estilow[c]

[a] Department of Statistics, University of Georgia, Athens, GA 30602, USA
[b] Department of Geography, University of Georgia, Athens, GA 30602, USA
[c] Department of Geography, Rutgers University, Piscataway, NJ 08854, USA

ARTICLE INFO

Keywords:
Columbia River Basin
Streamflow
Discharge
Remote sensing
Snow cover

ABSTRACT

In the western United States, meltwater from mountain snowpacks serves as the dominant water supply for many communities. Efficient distribution and use of this renewable, yet temporally and spatially variable resource relies critically on accurate forecasting of future water availability. Here we report on initial efforts to use Interactive Multisensor Snow and Ice Mapping System (IMS) data on snow coverage to forecast flow in six selected watersheds within the Columbia River Basin. Little research has been done on identifying the relationship between seasonal discharge volume and these satellite-derived snow cover data. In the Yakima watershed within the Columbia River Basin, we could explain 52% of the spring discharge (April – July total streamflow volume) variance by selecting specific 24-km grid cells that exhibit both strong correlation with historical flows as well as high inter-annual variation. This approach yielded reasonable success in other watersheds. Of the six Columbia River subbasins examined in this paper, five of them give statistically significant predictors of April – July streamflow volume at the $\alpha = 0.05$ level. When comparing this optimized specific-cell technique to the overall average across the entire watershed of interest, we observe improvements in each of our six subbasins, although in some regions, improvements were minimal. Clearly, this optimization technique is inherently limited by the role of snow cover variation in determining streamflow discharges in different subbasins. For both mountainous regions with extensive and stable snow cover as well as low-elevation regions with consistently minimal snow, the snow cover variation only accounts for a small inter-annual streamflow discharge variance. Our methodology shows that the IMS provides remotely-sensed data that are ready to "plug and play" into existing streamflow forecast models such as the Natural Resources Conservation Service's (NRCS) Visual Interactive Prediction and Estimation Routines (VIPER).

1. Introduction

As is true in much of the Pacific Northwest, snowpacks constitute a persistent central concern for people living in the Columbia River Basin (CRB). Meltwaters from these snowpacks provide the source water for the streams and rivers that drain throughout the basin, supplying the majority of water upon which the entire population relies (McCabe and Clark, 2005; Serreze et al., 1999). While these snowpacks are essential resources, they also constitute potential threats. In years of sparse snow accumulation, low-flow conditions can fall short of the region's water needs. By contrast, in years of ample accumulation, or during high rates of snow melt, high river flows can spur dangerous surges, flooding population centers, threatening lives, and destroying property (O'Connor and Costa, 2000; Historical High Water Events, 2014). Impacts of these extremes and the more common subtle inter-annual variations are of importance not just to public safety, but to irrigation, potable water, hydroelectric generation and, indeed, the overall economy of the Pacific Northwest (Mote, 2003). Hence, accurate streamflow predictions are a top priority in this region.

Snow cover plays a key role in the hydrologic cycle by acting as the frozen storage term in the water balance (Derksen and LeDrew, 2000). Thus, snow ablation is a major contributor to streamflow, soil moisture, and groundwater supplies. Every river basin has its own snow-ablation characteristics and melt-discharge relationships, with the Columbia River Basin and its subbasins (Fig. 1) being no exception. In this region, where snow cover can be deep and water-laden in the mountains, intra-seasonally ephemeral elsewhere, and where discharge exhibits notable inter-annual variability due to melt timing and snow-water content, forecasting of water release from the snowpack presents a formidable challenge. Such variability may lead to harmful environmental and

* Corresponding author.
E-mail address: bwash318@uga.edu (B. Washington).

https://doi.org/10.1016/j.rsase.2018.03.003
Received 31 August 2016; Received in revised form 12 December 2017; Accepted 13 March 2018
Available online 15 March 2018
2352-9385/

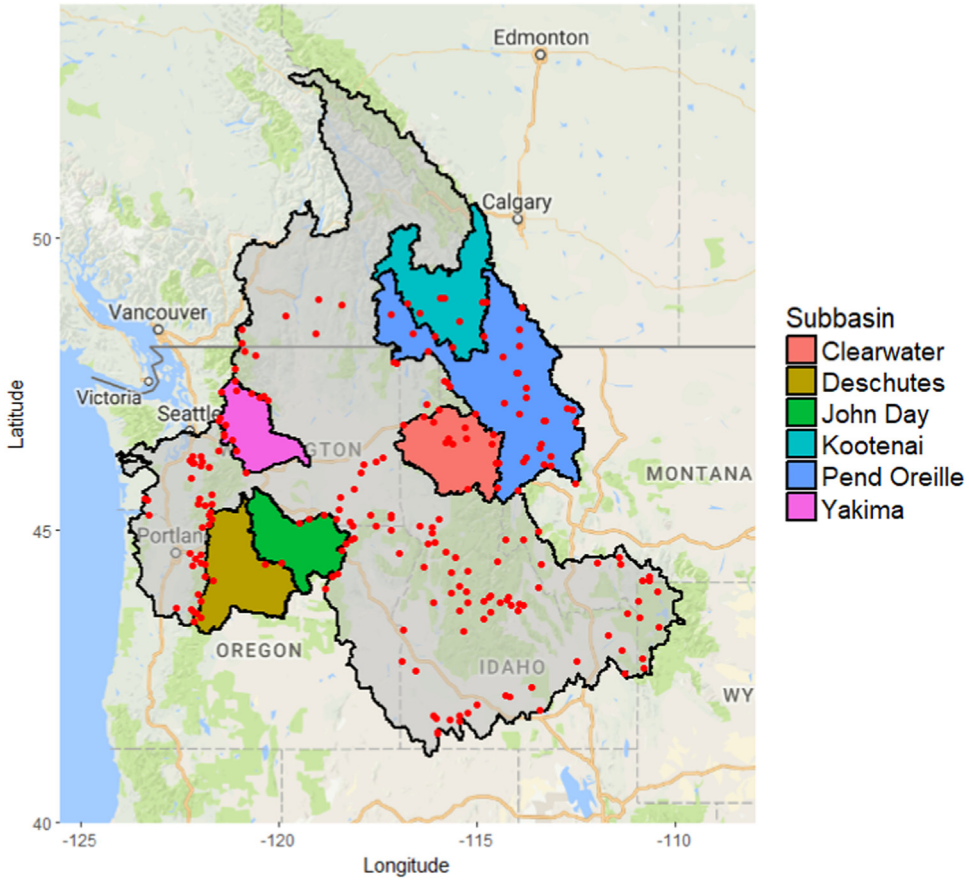

Fig. 1. The locations of US SNOTEL stations (red dots) superimposed on a map of the subbasins of interest. Note that the SNOTEL stations commonly are situated along subbasin boundaries, typically at or near geographic apices, where snow cover commonly is thicker and/or more persistent than lower elevations.

societal consequences, including snowmelt-induced floods, transport of pollutants or excess nutrients in rapid snowmelt events, and lack of adequate streamflow for irrigation, human consumption and power generation. Thus, accurate forecasting of water release from the snowpack is a requisite component of any accurate streamflow model in mountainous regions or other regions where snow is present.

Currently, forecasters at the U.S. Department of Agriculture National Resources Conservation Service (NRCS) Water Supply Forecasting Program use a program called Visual Interactive Prediction and Estimation Routines (VIPER) to make seasonal streamflow forecasts. These streamflow models are based on data retrieved from snow telemetry (SNOTEL) stations. SNOTEL stations provide snowpack-water content data via pressure-sensing snow pillows. Temperature, precipitation, and snow depth also are measured at these SNOTEL stations, which are distributed throughout much of the western United States. Because of the expensive nature and upkeep of SNOTEL stations, they are usually located in areas where snow cover is expected for a large portion of the year. SNOTEL sites are often in remote locations running along mountain ranges at high elevations. Fig. 1 shows the distribution of SNOTEL stations within the Columbia Basin. Sensor data are recorded every 15 min and transmitted from stations to a collection facility via meteor-burst technology. Example data for one of these SNOTEL stations are depicted in the Appendix (Fig. A1). While these SNOTEL data are temporally detailed, they are spatially sparse at the watershed scale and not intended to represent total snow across a basin (Gleason et al., 2016). Moreover, using solely these SNOTEL data to forecast streamflow inherently introduces bias as not all locations inside of the Columbia Basin tend to have as much snow as these exposed, high-elevation stations. Additionally, Nolin and Brown (2008) found that SNOTEL sites in the Willamette River Basin did not sample 50% of the elevation range that is typically snow covered. Within the CRB, SNOTEL sites sample elevations between 128 and 2902 m above sea level. Similar concerns with the basin-wide representativeness of SNOTEL locations have been explored at the headwaters of the Rio Grande River Basin (Molotch and Bales, 2006).

Here, we examine the utility of remote-sensing data in the prediction of seasonal streamflow volumes at selected forecast locations within the Columbia River Basin. Throughout the satellite era, observations of snow cover from various space-based instruments have been studied for their potential to enhance seasonal streamflow forecasts. For example, Rango et al. (1977) found that early meteorological satellites could be used to derive runoff estimates in the Himalayan region, with the potential to improve water resources management. Since this time, observations from the Landsat platform and instruments including the Special Sensor Microwave Imager (SSM/I) and Moderate Resolution Imaging Spectroradiometer (MODIS) have been used in studies of seasonal streamflow and its relationship to snow cover extent (e.g. Rango and Martinec, 1979; Zhou et al., 2005; McGuire et al., 2006; Andreadis and Lettenmaier, 2006; Nagler et al., 2008; Tong et al., 2010; Hall et al., 2012; Bergeron et al., 2014). It is important to note that

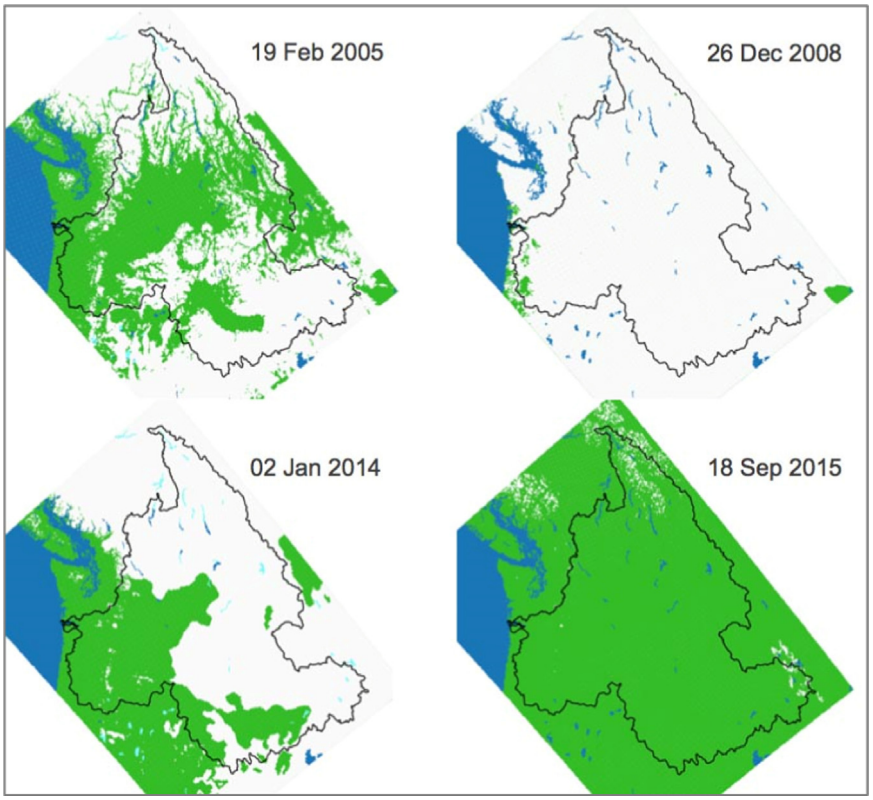

Fig. 2. Snow cover extent (SCE) within and adjacent to the Columbia Basin are shown on four selected dates within the IMS era. The maps depict grid cells at 4-km resolution that are 50% or more snow covered as white and those less than 50% covered (including those that are entirely snow free) as green.

cloud obscuration is limiting MODIS models. Many studies have been done to reduce the negative effect of cloud cover (Parajka and Blöschl, 2008).

Specifically, our study has utilized the latest generation of satellite-derived snow cover extent (SCE) data from the National Oceanic and Atmospheric Administration's National Environmental Satellite, Data and Information Service (NOAA/NESDIS) to determine whether this product may prove to be a useful tool in predicting spring streamflow discharge in the CRB. Historical NOAA/NESDIS-produced snow maps derived from visible satellite imagery have been recognized as a useful tool in the assessment of snow distribution in drainage basins (Rango, 1993). In other efforts analogous to the project described here, weekly SCE products from NOAA/NESDIS have demonstrated a strong relationship between streamflow and snow cover extents during the spring melt season in both large Siberian watersheds and the Yukon in northwest Canada (Yang et al., 2003, 2009). The working hypothesis is that using the rich array of remote-sensing SCE data will improve streamflow forecasting by decreasing the uncertainty, and perhaps spatial bias, introduced from the sparsely distributed SNOTEL stations. This hypothesis has been examined in the Upper Colorado River Basin, where studies have shown that the utilization of areal snow coverage information (from MODIS) has improved streamflow prediction (Liu et al., 2015). We propose a selection criterion to detect locations important in streamflow modeling, introduce a metric based on these locations, and analyze this metric's efficacy in selected subbasins with varying climates.

2. Materials and methods

2.1. Data sources

The primary observational data source in this study was the Interactive Multisensor Snow and Ice Mapping System (IMS), which is the latest generation in a joint effort from NOAA/NESDIS, the Naval Ice Center, and the United States Coast Guard. The joint product of these three federal organizations is called the National Ice Center (NIC).

Beginning in the late 1960s, weekly maps were generated by trained analysts who relied primarily on visible satellite imagery to make decisions regarding the presence or absence of snow or ice cover. These early maps were hand-drawn with the goal being simply obtaining the most accurate evaluation possible. Maps were then digitized using a 128 × 128 grid overlay of the polar stereographic projection (Robinson et al., 1993; Estilow et al., 2015). In late 1998, IMS mapping released its first operational daily product, a map gridded at about a 24-km resolution at 60°N latitude (Ramsay, 1998). Since then, these IMS maps have been generated daily, first by analysts at the NOAA/NESDIS Satellite Applications Branch and for the past decade at the NIC. In March of 2004, a higher resolution (4-km grid) product was introduced (Helfrich et al., 2007).

To understand the format of the IMS data, it is best to think of a square grid overlaid on top of a polar stereographic projection of the entire Northern Hemisphere (see Fig. A2). This grid is then stripped down to only include points within the Columbia River Basin. These grid points can be further reduced to any subbasin or watershed of interest within the Columbia system. IMS daily SCE values are binary (snow/no snow) for each pixel. Fig. 2 includes maps at the 4-km resolution for four dates that depict the wide range of snow cover conditions that may occur within the basin over the course of a season.

The IMS methodology facilitates the incorporation of data from multiple satellite and in situ sources, and includes interactive image analysis to better recognize regions covered by snow and ice from those lacking such covers (Helfrich et al., 2012). Despite the addition of more imagery and better analytic tools over the years, the product has consistently relied on trained analysts primarily evaluating visible imagery

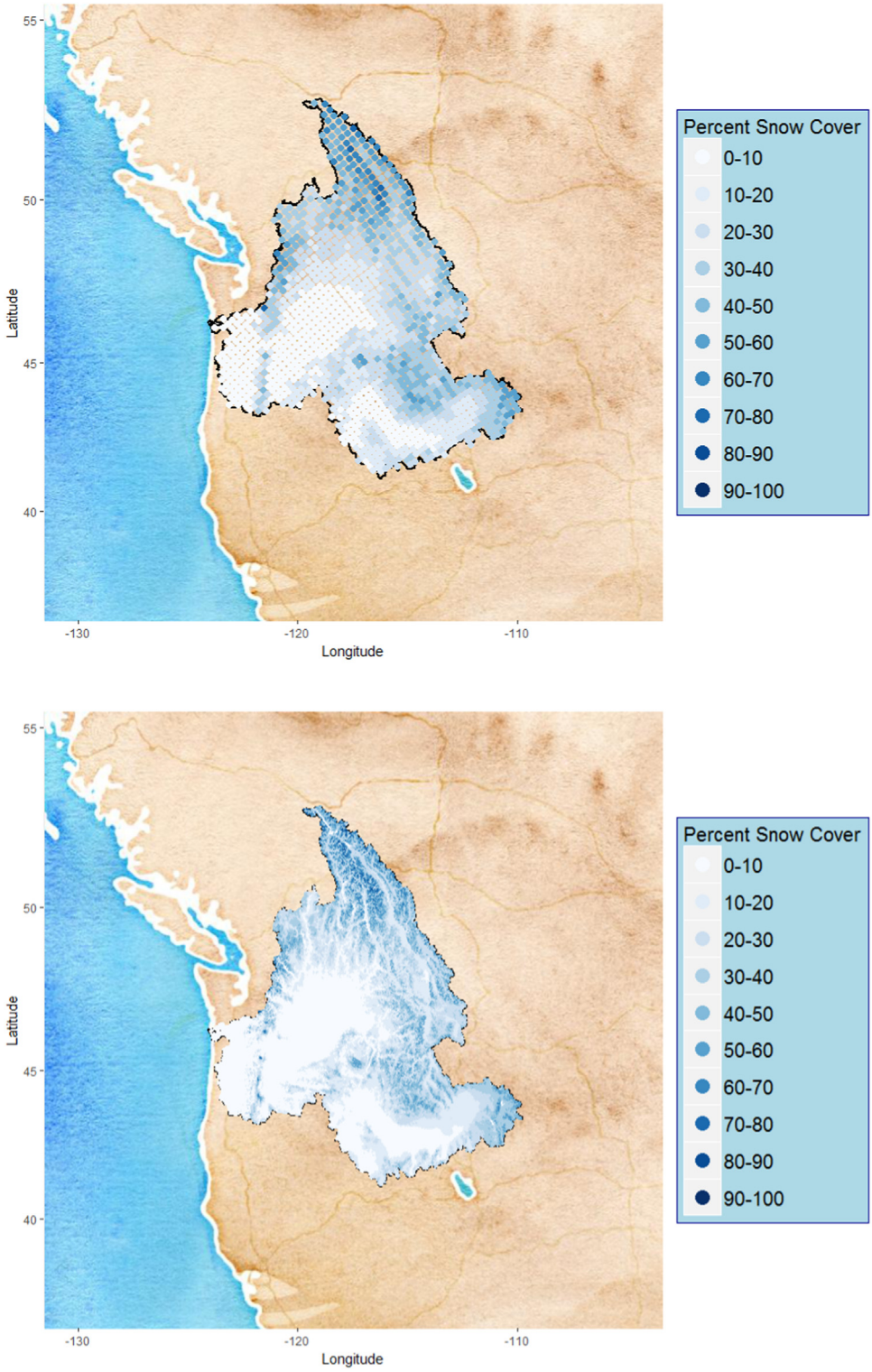

Fig. 3. The percent of days with snow cover in the Columbia River Basin based on 24-km resolution data (upper: 1999 – 2015) and 4-km resolution data (lower: 2005 – 2015).

to generate SCE maps. Both the 24-km and the 4-km IMS resolutions used in this study can be accessed from the National Snow and Ice Data Center (National Ice Center, 2008).

Fig. 3 displays this spatial variability in SCE over the entire region during the course of the IMS era. In Fig. 3, we see the percent snow cover across the basin from 1999 to 2015 for the 24-km resolution (top) and from 2005 to 2015 for the 4-km resolution. While not covering a typical 30-year climatological interval, these analyses demonstrate the considerable spatial variation in SCE, which is clearly a strong function of elevation as well as latitude.

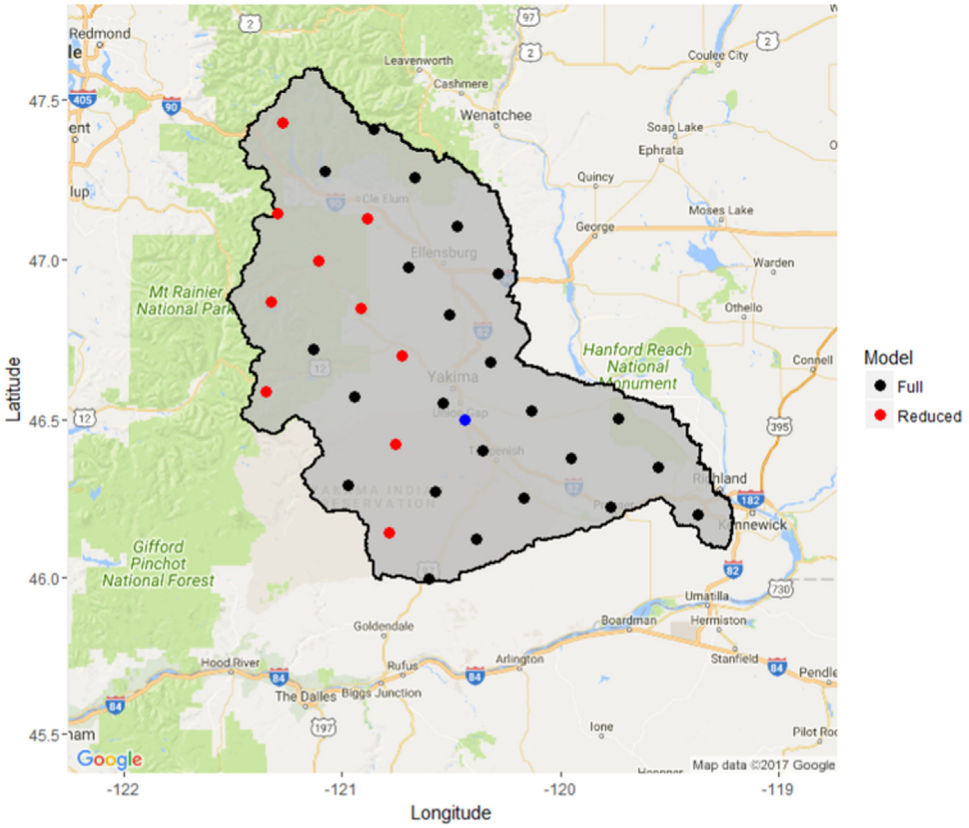

Fig. 4. Yakima subbasin shown with the IMS 24-km locations in the full model (black and red dots), the IMS 24-km locations in the reduced model (red dots), and the USGS gauging location at Yakima Parker (blue dot).

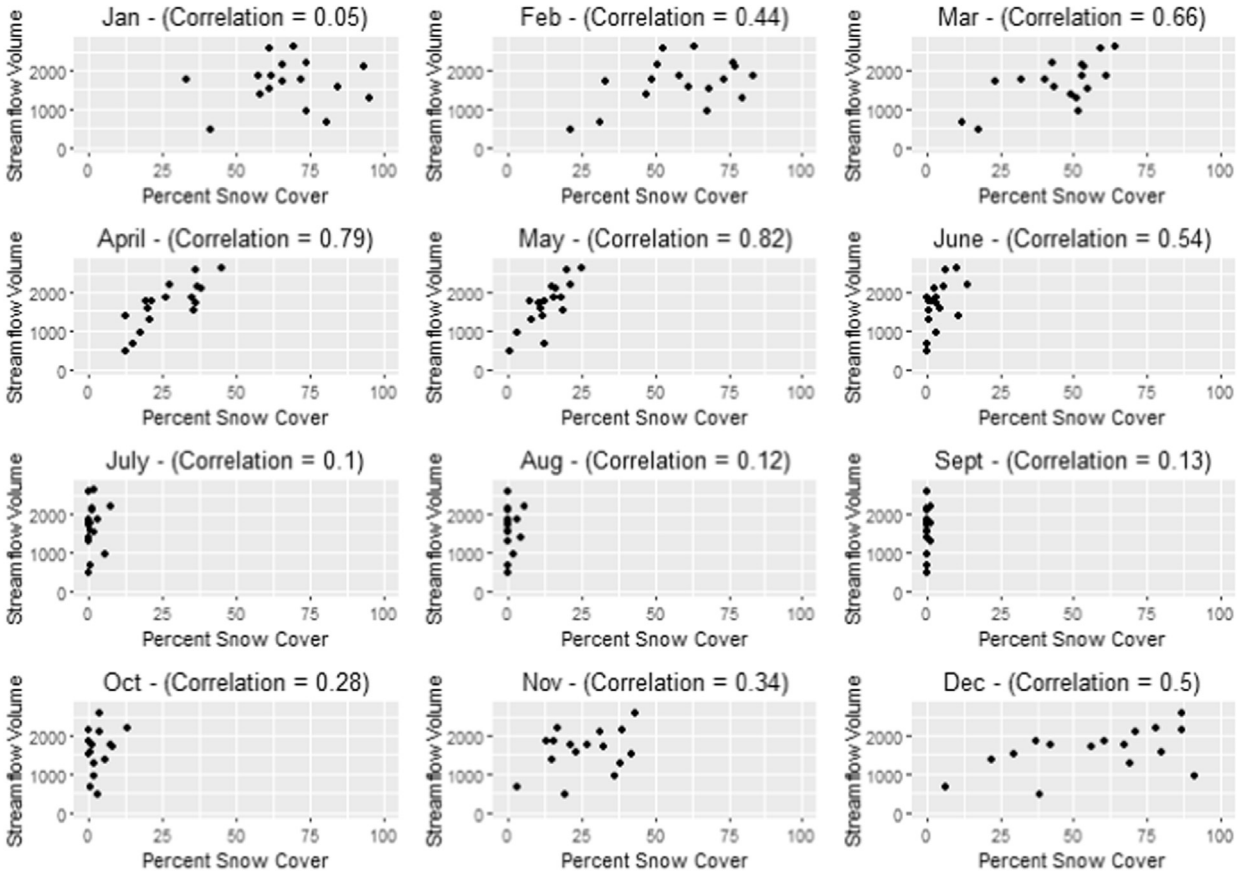

Fig. 5. April to July streamflow volume in the Yakima basin as a function of the average February – March *PSC*.

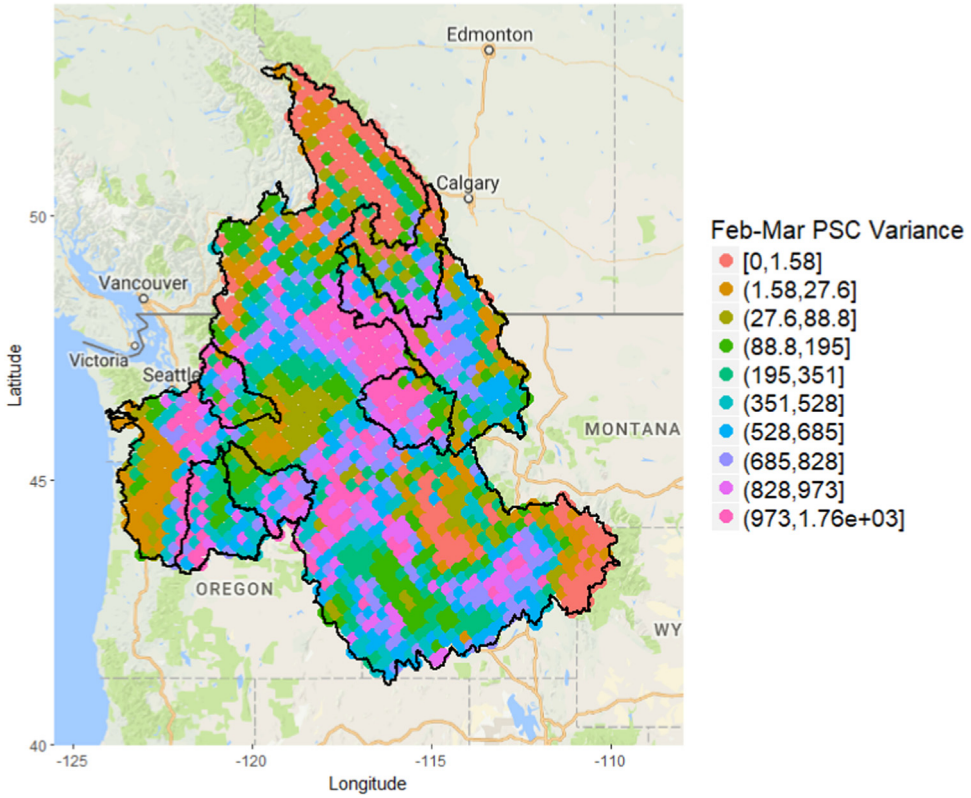

Fig. 6. February to March PSC variance for all 24-km IMS grid cells in the Columbia River Basin along with outlines of subbasins of interest.

Table 1
Selection criteria for each of the subbasins of interest.

Subbasin	Feb – Mar Full *PSC* 50th percentile variance	Feb – Mar Full *PSC* 50th percentile correlation
Yakima	519.63	0.46
Deschutes	548.90	0.48
John Day	579.03	0.42
Clearwater	830.28	0.49
Pend Oreille	567.91	0.39
Kootenai	129.12	0.32

As noted earlier, and depicted in Fig. 3, this gridded product exists in two formats, at 24-km and 4-km resolution. At first glance, it seems as if the higher resolution product would provide a more powerful predictive tool than the lower resolution. However, there are several notable tradeoffs associated with this increase in resolution. The most significant of these tradeoffs is that the 4-km data only dates back to March 2004, whereas the 24-km data extends back to January 1999. Because our period of record is relatively short, we decided to employ the lower resolution IMS product only, the daily 24-km product, although we do examine the effectiveness of the 4-km product in the Yakima subbasin. We believe that the 24-km product provides the spatial and temporal resolution appropriate for an initial investigation within the basins of the Columbia system, while at the same time not sacrificing a critical five years of prediction power.

We compare IMS snow cover to measured streamflow discharge. Streamflow is recorded at thousands of gauging stations throughout the nation by the United States Geological Survey and freely available online (U.S. Geological Survey, 2012). The distribution of stream gauges within the Deschutes subbasin is shown in Fig. A3, along with discharge data for two separate gauging stations from September 2009 to August 2010. We can see that only a few SNOTEL stations lies within the Deschutes subbasin. Many nearby SNOTEL stations are located just

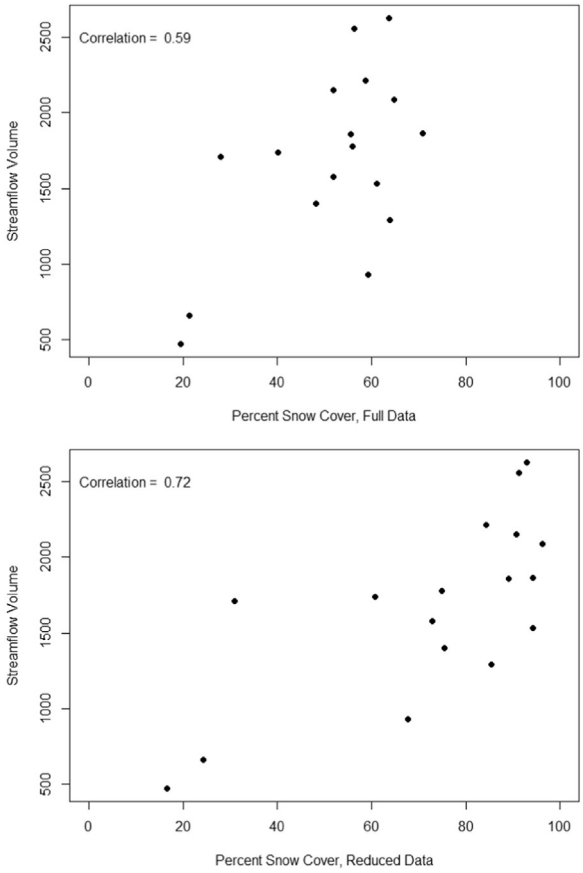

Fig. 7. Full *PSC* (top) and Reduced *PSC* (bottom) versus the Yakima Parker streamflow volume (1999–2015).

Table 2
Comparison of the February – March reduced *PSC* to that of the March reduced *PSC* linear regression models in the all six subbasins.

	Feb-March snow signal		March snow signal		
	R^2	P-value	R^2	P-value	Degrees of freedom
Yakima Full	0.35	0.0124	0.42	0.0047	15
Yakima Red.	0.52	0.0012	0.56	0.0006	15
Deschutes Full	0.52	0.0017	0.64	0.0002	14
Deschutes Red.	0.63	0.0002	0.69	0.0001	14
John Day Full	0.30	0.0232	0.29	0.0245	15
John Day Red.	0.34	0.0146	0.39	0.0075	15
Clearwater Full	0.31	0.0204	0.35	0.0118	15
Clearwater Red.	0.35	0.0119	0.41	0.0053	15
Pend Oreille Full	0.24	0.0462	0.33	0.0158	15
Pend Oreille Red.	0.25	0.0412	0.34	0.0138	15
Kootenai Full	0.16	0.1097	0.17	0.0997	15
Kootenai Red.	0.17	0.0963	0.19	0.0810	15

Table 3
The inter-annual median variances of the reduced *PSC*, where *PSC* metrics are based off of February – March as well as March, alone.

Subbasin	Feb-March median variance	March median variance
Yakima	998.49	1137.45
Deschutes	1021.32	1750.78
John Day	877.45	1105.59
Clearwater	1004.20	1268.90
Pend Oreille	812.78	1258.98
Kootenai	831.32	1161.02

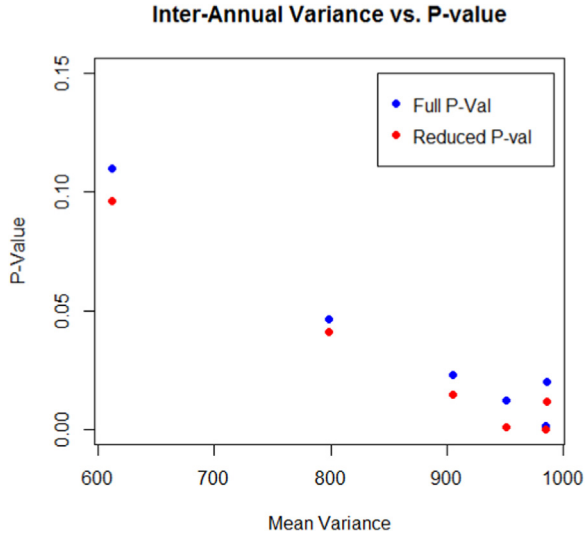

Fig. 8. Mean inter-annual variance vs. full (blue) and reduced (red) p-values for each of our six subbasins. (For interpretation of the references to color in this figure legend, the reader is referred to the web version of this article)

west of this watershed. Consequently, this would make it difficult to use SNOTEL as a predictor for streamflow at these gauging sites. This provides perspective regarding the spatial paucity of SNOTEL sites when looking within specific subbasins. Given the low density and relative distribution of SNOTEL sites, one might assume that the streamflow prediction at many of these gauging stations may not be directly related to measurements recorded at the SNOTEL locations.

2.2. Method development

To present our methodology, preliminary analyses are restricted to the 24-km product inside of the Yakima subbasin (Fig. 4). Once we have defined our method, we will examine its performance in other subbasins. All of our analyses focus only on the critical spring discharge season, April – July, when snowmelt often is at its highest, and snowpack distribution and morphology is most transient and challenging to characterize.

As a first round of exploration into the utility of snow cover as a predictor for streamflow volume, a generic metric of percent snow cover is defined from the 24-km IMS satellite data using the following formula.

$$PSC = 100^{*}\frac{1}{N}\sum_{n=1}^{N} x \tag{1}$$

Here, N is the total number of days of interest in our prediction time frame, and x equals 1 if that grid point is under snow cover and 0 if that grid point is uncovered. Therefore, at each IMS location, *PSC* simply represents the percentage of days under snow cover for a given time window.

Intuitively, it seems as if the best time window for employing a snow-based metric to predict April – July streamflow volume would be immediately preceding or during these months. In Fig. 5, we explore this thought a bit more. Using Eq. (2) below, we create a spatial mean *PSC* metric.

$$SpatPSC = \frac{1}{N_2}\sum_{r\in R} PSC \tag{2}$$

This new metric, *SpatPSC*, is simply the average of all *PSC* values within a certain region, R. In Fig. 5, we examine the relationship between each month's *SpatPSC* value and the April – July streamflow volumes inside of the Yakima subbasin. In Fig. 4, the black and red points represent each IMS location of which *SpatPSC* is based, and the blue point indicates the location of the streamflow gauge. For the months August – December, we predict the upcoming season's discharge, as this is the period during which snow begins accumulating for the season. Consequently, in Fig. 5, the months from August to December have one less data point than other months, as we do not have a discharge volume for 2016. Hence, there are 17 years (1999–2015) of prediction for the months January – July, but only 16 years (1999–2014) of prediction for the months August – December. With correlation coefficients less than 0.3, we see that the months July – October as well as January may have little value in April – July discharge prediction. Correlations are highest in April and May, indicating that these months would be could predictors for total spring discharge. This is to be expected as these months fall within the forecast period. Ideally, however, a strong signal could be detected from months preceding the spring forecast period and therefore we will focus on February and March.

Next, we argue that these IMS data may be more “signal-rich” when a large fraction of grid points is neither primarily snow covered for a large portion of the year nor primarily snow free for a large portion of the year. It is difficult to extract an instructive signal from data that is primarily constant for a large portion of the year, thus this method might work better by selecting grid points that document a snowpack that builds up and then recedes seasonally.

One way to attack this issue is to examine certain regions within a basin that experience more variability in snow cover than others. As

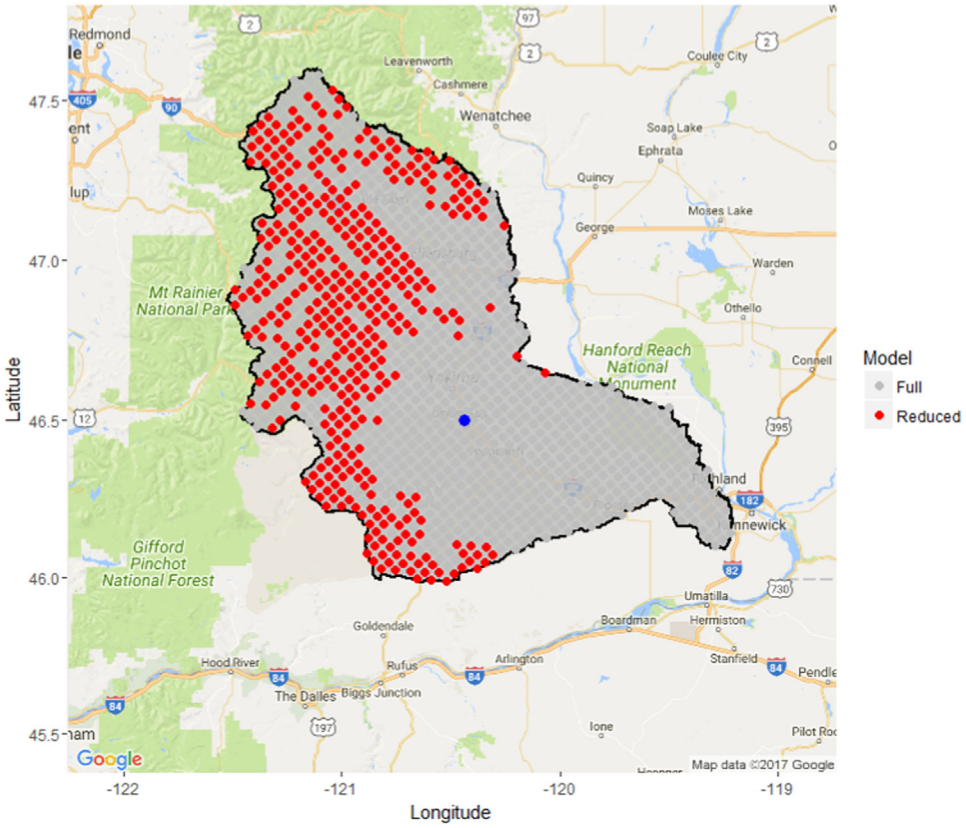

Fig. 9. Yakima subbasin shown with the IMS 4-km locations in the full model (gray and red dots), the IMS 24-km locations in the reduced model (red dots), and the USGS gauging location at Yakima Parker (blue dot). (For interpretation of the references to color in this figure legend, the reader is referred to the web version of this article)

Biggs and Whitaker (2012) found in the Merced River Basin, ablation may be occurring within critical elevation zones that shift during the season, dominating melt volumes. We note the elevation range sampled via our 24-km IMS data is within 0 and 3781 m above sea level (a larger elevation range than is sampled by SNOTEL alone). For example, many of the higher elevations inside of a Columbia subbasin are primarily snow covered for many months of the year, if not year-round, whereas lower elevation cells will be primarily uncovered, even throughout much of the winter. What makes prediction even more difficult is that, often, cells that remain constant throughout a given year will remain constant inter-annually. In contrast, grid points at these critical elevations (Biggs and Whitaker, 2012) might be expected to have more variability in snow extent within a season and more notably, inter-annually. In Fig. 6, we display a map of the inter-annual February – March *PSC* variance at the 24-km resolution. Identification and examination of these key areas might make it easier to recognize an effective predictive discharge signal for the basin. Essentially, when looking at the average across an entire subbasin, the strength of the discharge signal that might have been extracted from these critical elevation IMS grid cells is being diluted by the noise of less variant IMS locations.

Given the objective of selecting points that are highly correlated with spring discharge as well as high inter-annual SCE variability, we: i) find the correlation of each IMS location's February – March *PSC* with discharge; ii) calculate each location's inter-annual variance in February – March *PSC*; and iii) select those points that are in the top 50th percentile in both correlation and variance (values larger than the statistics reported in Table 1). Again, the motivation for utilizing the February – March prediction period is that the months immediately preceding the streamflow season should be most instructive regarding the upcoming spring discharge. The red points in Fig. 4 indicate the 10 locations that met the dual criteria of being in both the top 50th percentile for variance as well as the top 50th percentile for correlation with streamflow.

Fig. 7 depicts scatterplots comparing *PSC* to streamflow for both the full *PSC* (all 33 IMS points) and the reduced *PSC* (10 selected IMS points). Comparing the unfiltered to the filtered data (Fig. 7), it can be deduced that much of the Yakima basin must be primarily uncovered for a large portion of our February – March prediction timeframe. Specifically, this can be seen from the rightward shift in the data points in our reduced scatterplot in Fig. 7(i.e. the reduced data sees higher percent SCE in February and March). Simple linear regression of *PSC* to predict Yakima Parker streamflow volume (Table 2: Feb-March Snow Signal) documents a substantial improvement in the strength of our signal using the reduced model.

3. Results and discussion

3.1. Examination of the utility of the 24-km product in other subbasins

Here, we compare the performance of our "select cell" method to that of the overall *PSC* average in five other subbasins and discuss improvements that could be made to our model. Recall that our explanatory variable is the mean of certain IMS *PSC* values from February 1 to March 31. The full *PSC* signal is based on the entire set of IMS sample locations within our subbasin of interest. Whereas the reduced signal is based only on the IMS locations which exhibit both large correlation between the February – March *PSC* and total spring discharge as well as large February – March *PSC* variance.

We proceed to the Deschutes subbasin (Fig. 1). In this particular subbasin, the streamflow gauging location went offline in September

2014, so the prediction period is from 1999 to 2014. Here, the full *PSC* signal is based on 58 IMS sample locations, whereas the reduced *PSC* signal includes only 18 IMS sample locations (Fig. A4). The results for the Deschutes subbasin are summarized in Fig. A5 and Table 2 (Feb-March Snow Signal). Again, we see a rightward shift in the reduced-data scatterplot indicating that the basin is primarily uncovered when compared with our selected cells. We also note a substantial improvement when regressing discharge against the reduced signal compared to that of the full data, although both are highly statistically significant.

Now, we consider the adjacent river subbasin, John Day (Fig. 1). This subbasin spans a smaller area than does the Deschutes. The full *PSC* metric is based on all 47 IMS locations inside this region, while the reduced signal only includes 16 IMS locations (Fig. A6). Fig. A7 and Table 2 (Feb-March Snow Signal) show that the methodology presented here did not perform as well in this subbasin, although there is still an improvement in using the reduced signal.

The final three subbasins (Clearwater, Pend Oreille, and Kootenai, Fig. A8, A10, and A12, respectively) are clustered in the eastern portion of the CRB. The results are very similar for these subbasins. Again, Table 2 (Feb-March Snow Signal) displays the results of the linear regression models for these three subbasins as well. In each of these three subbasins, the R^2 improvements were minimal. The p-values were significant for both the full and reduced models in both the Pend Oreille and Clearwater subbasins at the $\alpha = 0.05$ level. The Kootenai was the only subbasin that did not yield a statistically significant effect in either of the full or reduced signal's at the $\alpha = 0.05$ level. All other subbasins saw a significant effect in both the full and reduced signals.

Why did the reduced model have such a large improvement in both the Yakima and Deschutes subbasins in comparison with our other four watersheds? We hypothesize that our February – March *PSC* signals have relatively low inter-annual variance in these four regions. Note that a low inter-annual *PSC* variance would indicate that our snow signal is not changing much from year to year. This would imply that it would be difficult to differentiate between low and high seasonal discharge as our signal is somewhat constant. Table 3 (Feb-March) displays the median inter-annual variances for the six subbasins of interest. Fig. 8 is a plot of our mean inter-annual variances against the full and reduced p-values for the six subbasins. There does appear to be a negative relationship between inter-annual variance and the significance of our signal, where higher variances tend to have lower p-values.

The two subbasins for which our *PSC* metric performed the worst (Kootenai and Pend Oreille) had the lowest variances among the six subbasins. Somewhat surprisingly, the Clearwater region had a high median variance (Table 3: Feb-March). Also, Figs. A8, A10, and A12 indicate that the Clearwater, Pend Oreille, and Kootenai subbasins (located in northern Idaho, northwestern Montana, and Alberta) tend to have more snow cover than the Yakima, Deschutes, and John Day subbasins. Perhaps this February – March prediction period does not provide enough inter-annual variability in these rather snowy regions. On the other end of the spectrum, the John Day region, in central Oregon, sees much less snow than the Pend Oreille, Clearwater and Kootenai watersheds. The relatively small improvements in the reduced model in this region could again be caused by a lack of inter-annual variation in snow cover in February and March; this time, however, the basin is consistently seeing very little snow.

3.2. Examination of the utility of the 24-km product for a March prediction period

In this section, we discuss the utility of an alternative *PSC* prediction period: one that is based entirely on March. We expect that in our snowier subbasins (Clearwater, Pend Oreille, and Kootenai), we would have more variation in snow cover over just March as opposed to February and March together. In Table 3, we note that our median inter-annual reduced *PSC* variances have increased when we restrict our timeframe to just March in each of the six subbasins. In Table 2, we see that in every case except one (John Day Full), our p-values have decreased and R^2 values have increased with this new March *PSC* metric which sees higher variations. For each subbasin, it is important to note that the reduced models may be based on different sets of locations. This makes sense as locations which see high February – March variability may not see high March variability and vice versa.

Again, our reduced *PSC* metric significantly outperformed our full *PSC* metric in the Yakima subbasin. With the March *PSC* metric, however, the John Day subbasin saw substantial improvements in the R^2 value in the restricted model. We observed a moderate improvement in R^2 when using the reduced metric in both the Deschutes and Clearwater subbasins. Improvements were again minimal in both the Pend Oreille and Kootenai subbasins. As each subbasin sees its own climate and snow patterns, we expect the optimal time window to differ across subbasins. Further studies could be done on *PSC* time optimization for each subbasin.

3.3. Examination of the 4-km product in the Yakima subbasin

In this section, we report on a primary investigation into the IMS 4-km product for only the Yakima subbasin. Despite the increased prediction power of the March *PSC*, we return to the original February – March prediction period to compare the results to that of the 24-km product. We note that in 2004, we have used only March *PSC*, as IMS 4-km data does not exist before March of 2004. In Fig. 9, we present a map of the new IMS locations of the full *PSC* metric (red and gray points) as well as the reduced *PSC* metric (red points only). Comparing Fig. 4 to Fig. 9, we see that similar regions within the Yakima subbasin meet our dual criteria of high correlation between February – March *PSC* and streamflow volume as well as high February – March *PSC* variance at both spatial resolutions.

As before, we regress the full and reduced PSC metrics to the total spring streamflow discharge. The full and reduced models have p-values of 0.0097 and 0.0015 with R^2 values of 0.50 and 0.65, respectively. The results are very similar to that of the 24-km product (Table 2) indicating that the 24-km product is sufficient. We restate that the major motivation for using the 24-km product is that it is based on a longer historical record (1999–2015) compared to that of the 4-km product (2004–2015).

4. Conclusions

These results indicate that in most of the tested areas within the CRB, a simple temporal *PSC* average built using the IMS remotely sensed snow cover data provides a statistically significant predictive model of April – July seasonal discharge volume. In only one (Kootenai; p-value of 0.110) of the six subbasins examined were the results not statistically significant at the $\alpha = 0.05$ level for our February – March signal. When restricting our models to include only locations with relatively high correlation and variation, we saw notable improvements in prediction power.

All of the restricted February – March *PSC* models were significant at the $\alpha = 0.10$ level, with the Kootenai subbasin being the only reduced model not significant at the $\alpha = 0.05$ level (p-value of 0.096). However, in many of these subbasins (John Day, Clearwater, Pend Oreille) we note that our reduced *PSC* metric did not substantially outperform our full data *PSC* metric. In the Yakima and Deschutes

subbasins, the reduced *PSC* metric saw a substantial improvement over that of the full *PSC* metric, although both metrics saw statistically significant results at the $\alpha = 0.05$. When restricting the scope of our reduced *PSC* metric to just March alone, we saw increased variations in all six of our subbasins. Consequently, we saw an increase in predictive power in every reduced model. We believe that each subbasin will exhibit its own optimal temporal *PSC* metric based, related to elevation, climate, and snowmelt-discharge patterns. We reiterate that improvements in prediction power are inherently restricted by the role of snow cover variation in determining river discharge. In some subbasins, snow cover variation will have a much larger role than in others.

Our methodology shows that IMS provides remotely-sensed data that are ready to "plug and play" into an existing streamflow forecast model such as NRCS VIPER. Using IMS-derived SCE alongside inputs currently used by VIPER has the potential to improve CRB streamflow predictions. One advantage to using IMS SCE with an existing prediction tool such as VIPER is its operational nature. IMS forward processing will continue, and as the temporal record increases in length, forecast success is expected to improve.

The results of these analyses show that seasonal streamflow discharge can be related to these satellite-derived IMS SCE data in the Columbia River Basin. However, utility of IMS for streamflow forecasting appears not to be uniform across the entire region; it may be some function of location, climate, and elevation. Future analyses could explore the optimization of time period for the *PSC* metric, different selection criteria, or analyze the impact of utilizing some sort of combination of both SNOTEL stations and these IMS data. More advanced models could also include north-south slope and aspect features and their effects on snow melt and timing of peak streamflow – in the Northern Hemisphere, south facing slopes receive less sun radiation than do north facing slopes (Kumar et al., 2013). An ideal model would utilize elevation data, IMS data, and SNOTEL snowpack measurements to interpolate and estimate the amount of snow on the ground at each IMS grid location (as these locations are far more abundant than SNOTEL locations). This could be used to recognize possible peak streamflow events (i.e. when temperatures move above freezing in areas where the snowpack is estimated to be particularly dense) and predict how much water will be melting off of that particular snowpack.

Acknowledgements

This work was supported by the NOAA National Centers for Environmental Information (NOAA/NCEI) and Global Science and Technology, Inc. (GST). We thank DeWayne Cecil, who had the insightful vision that spawned this study. Our team included investigators Philip Mote and Kathie Dello (Oregon State University) in addition to the authors of this study, and we thank our Oregon State colleagues for their contributions. We are also indebted to individuals from several agencies who contributed their valuable time and tremendous expertise to this project. Those individuals include Taylor Dixon from the National Weather Service Northwest River Forecast Center in Portland, Oregon, Kyle Dittmer from the Columbia River Inter-Tribal Fish Commission, and especially Rashawn Tama from the U.S. Department of Agriculture Natural Resources Conservation Service. Many of the figures in this paper were created with the R-package 'Ggplot2' (Wickham, 2009).

Appendix

See Figs. A1–A13 here.

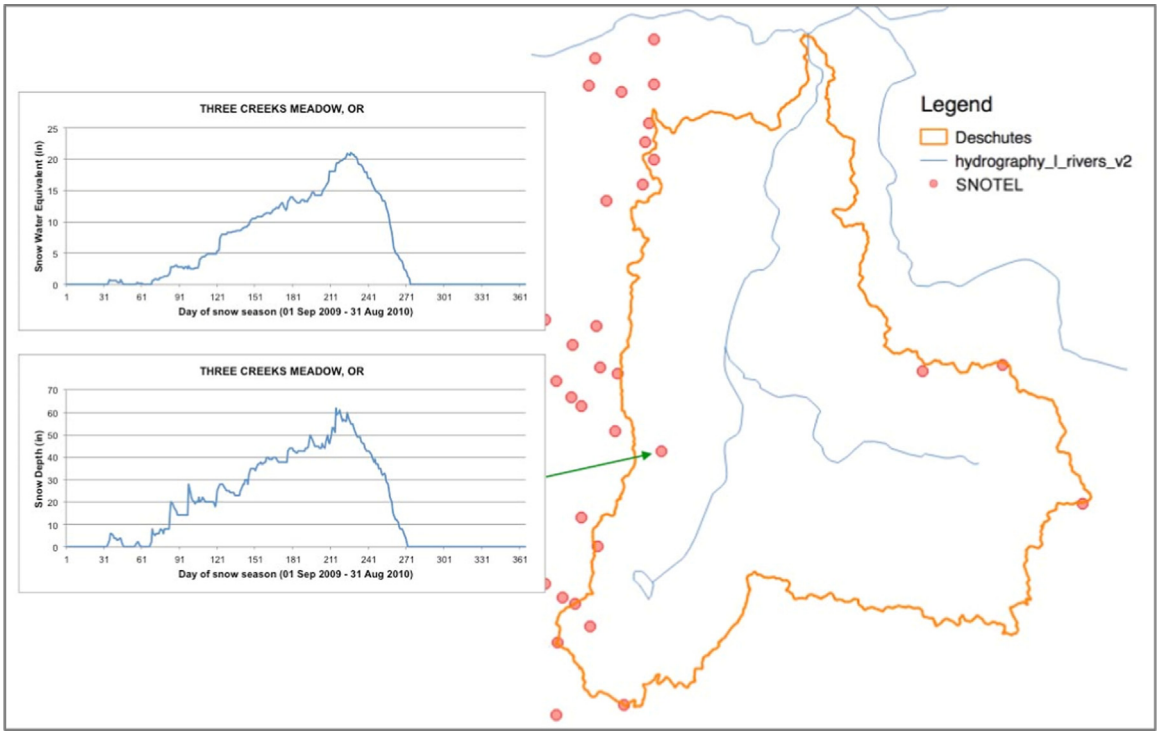

Fig. A1. Snow cover extent (top) and snow depth (bottom) for the Three Creeks Meadow, Oregon SNOTEL station (location shown on map) from 1 September 2009–31 August 2010.

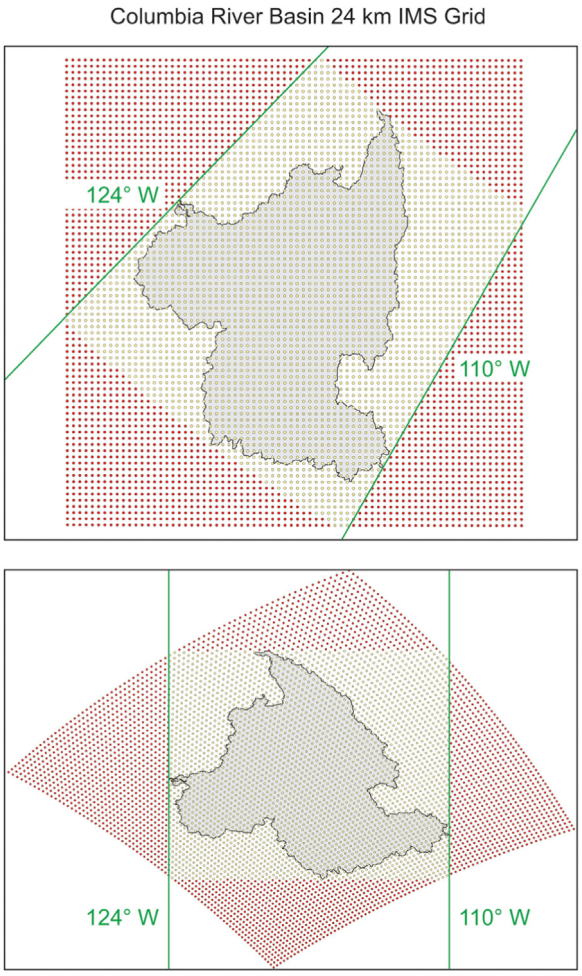

Fig. A2. The 24-km IMS grid coordinates in polar stereographic projection (top) and equirectangular projection (below) over the Columbia River Basin.

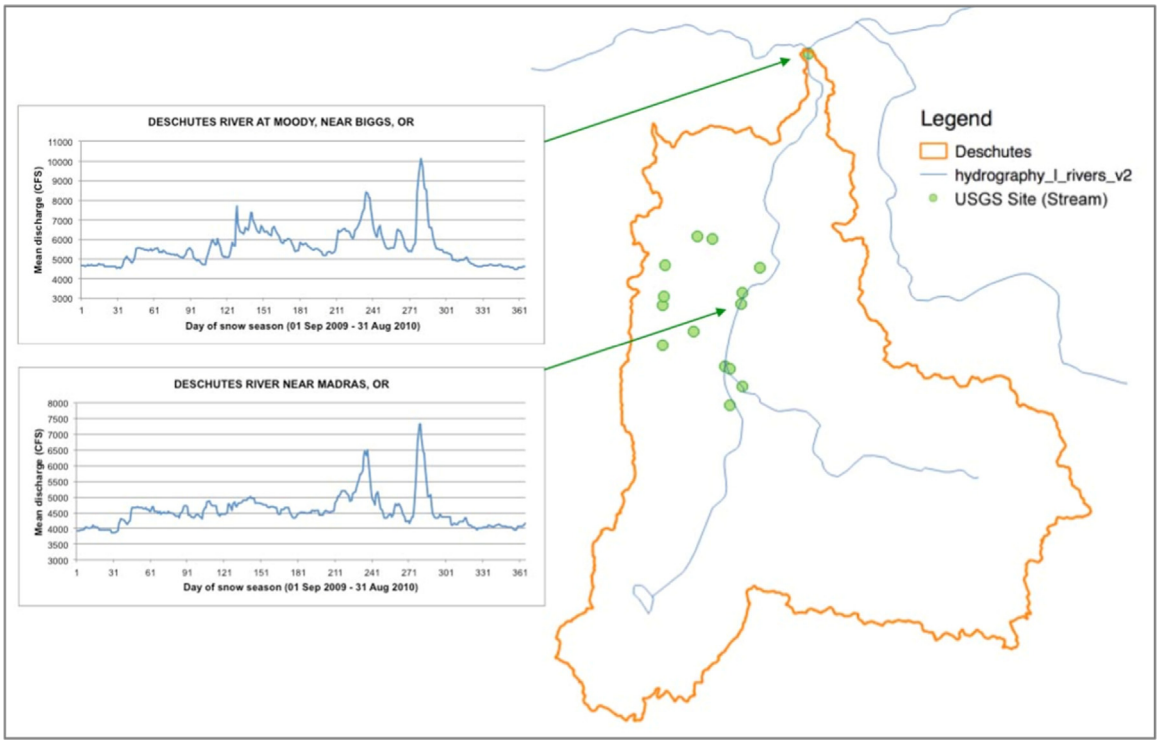

Fig. A3. Stream discharge observations (cfs) at two USGS gauging stations on the Deschutes River, Oregon from 1 September 2009 to 31 August 2010.

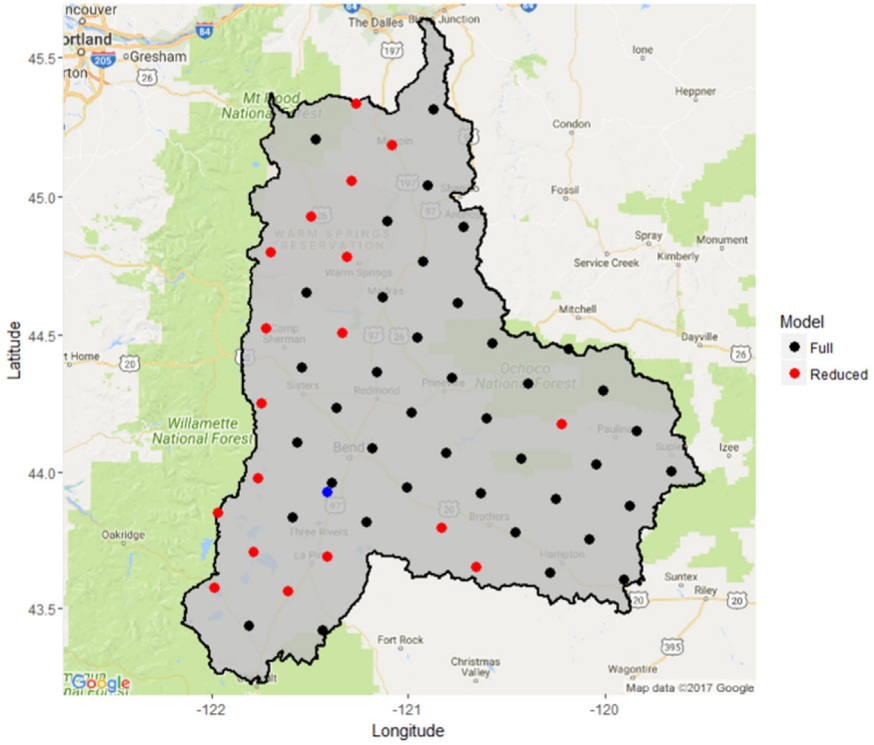

Fig. A4. IMS sample locations in the Deschutes subbasin for the Full *PSC* metric (black and red dots) as well as Reduced *PSC* metric (red dots).

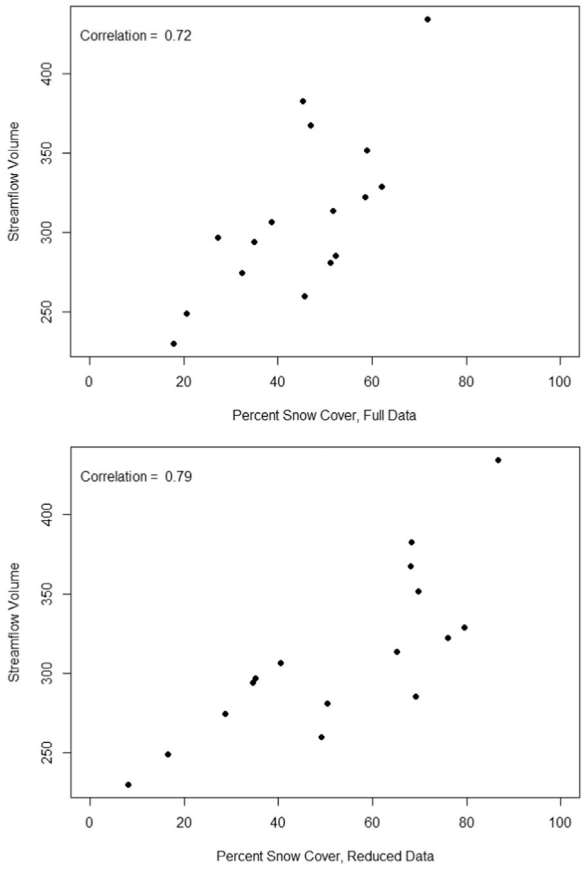

Fig. A5. Full *PSC* (top) and Reduced *PSC* (bottom) shown versus Deschutes River Benham Falls streamflow volume (1999–2015) with the correlation shown in scatterplot.

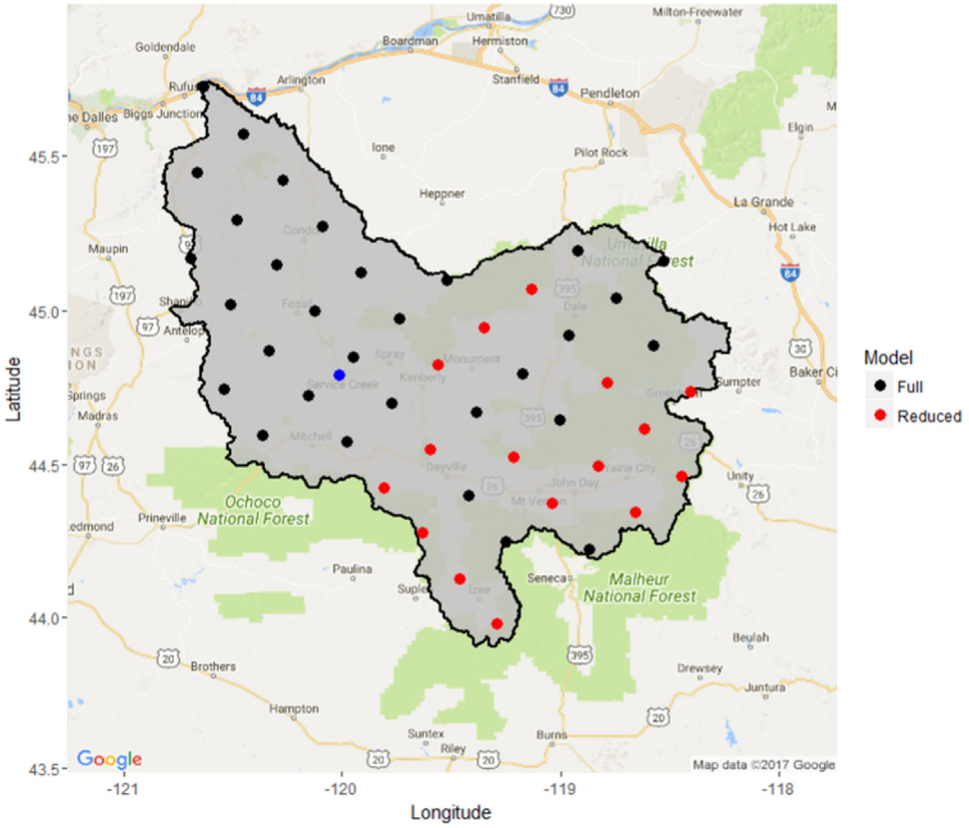

Fig. A6. IMS sample locations in the John Day subbasin for the Full *PSC* metric (black and red dots) as well as Reduced *PSC* metric (red dots). (For interpretation of the references to color in this figure legend, the reader is referred to the web version of this article)

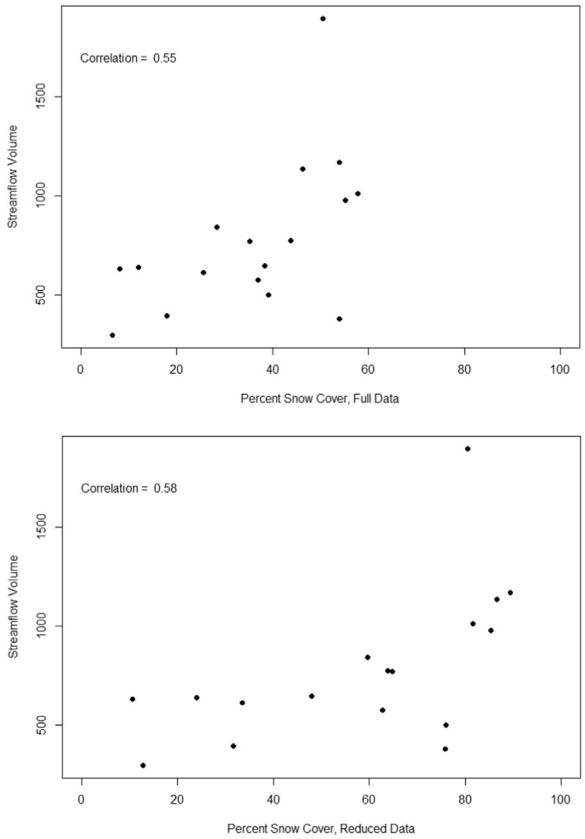

Fig. A7. Full *PSC* (top) and Reduced *PSC* (bottom) shown versus John Day River Service Creek streamflow volume (1999–2015) with the correlation shown in scatterplot.

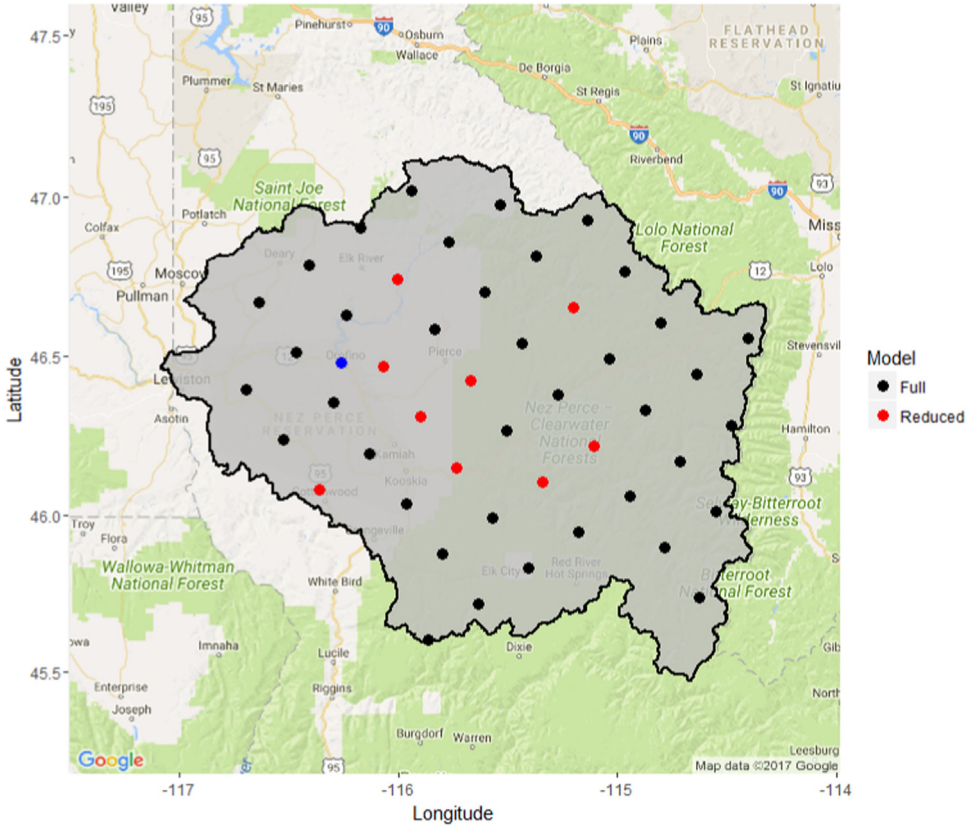

Fig. A8. IMS sample locations in the Clearwater subbasin for the Full *PSC* metric (black and red dots) as well as Reduced *PSC* metric (red dots). (For interpretation of the references to color in this figure legend, the reader is referred to the web version of this article)

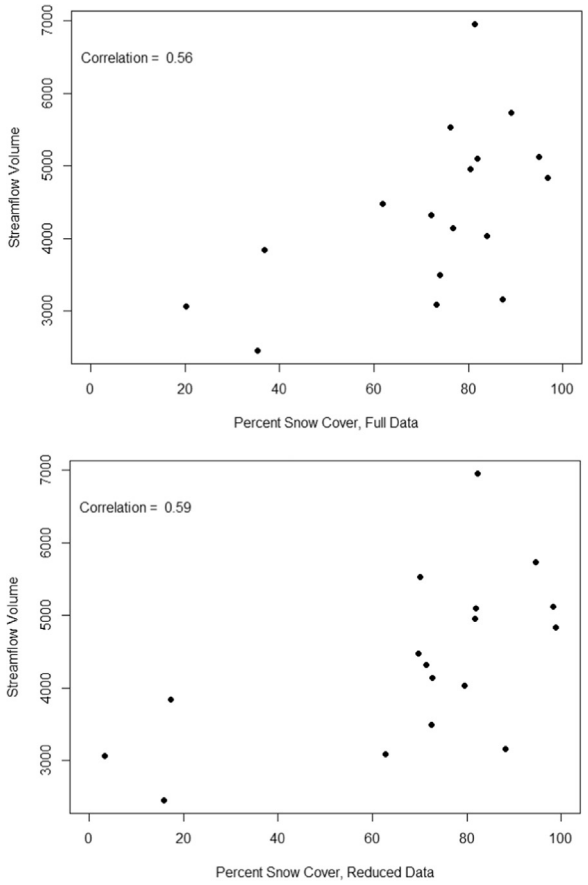

Fig. A9. Full *PSC* (top) and Reduced *PSC* (bottom) shown versus Clearwater River at Orofino streamflow volume (1999–2015) with the correlation shown in scatterplot.

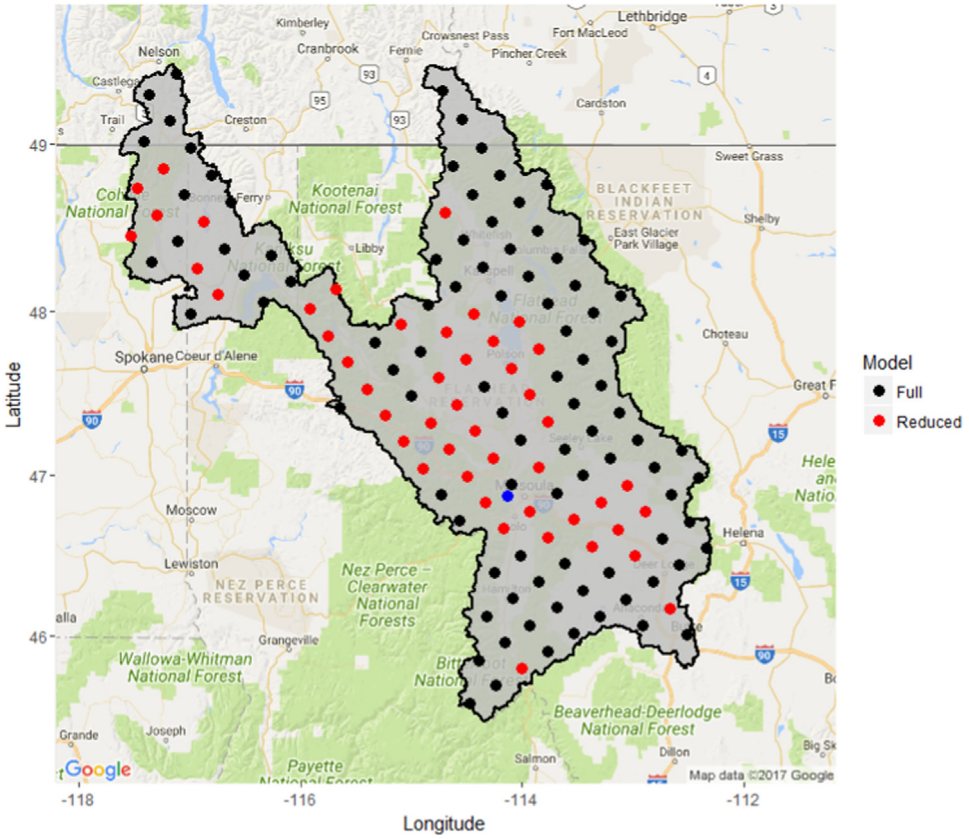

Fig. A10. IMS sample locations in the Pend Oreille subbasin for the Full *PSC* metric (black and red dots) as well as Reduced *PSC* metric (red dots). (For interpretation of the references to color in this figure legend, the reader is referred to the web version of this article)

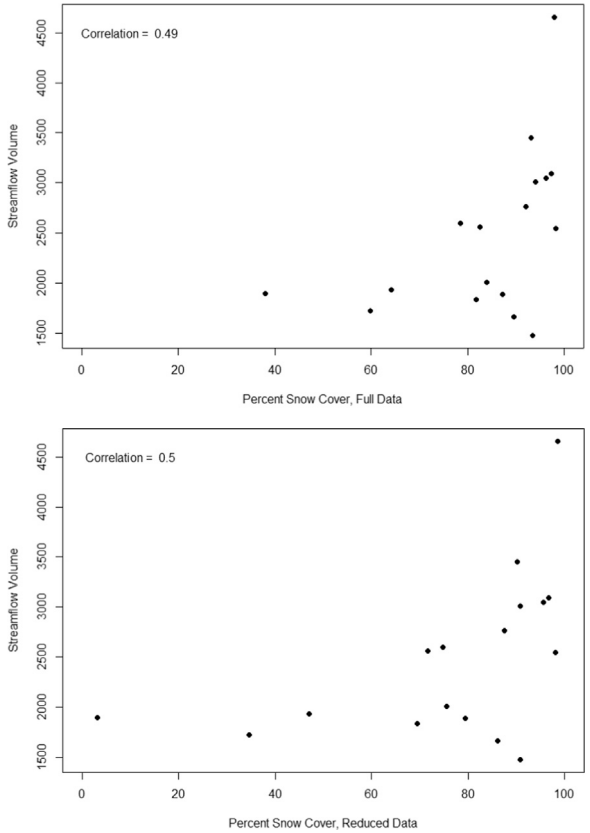

Fig. A11. Full *PSC* (top) and Reduced *PSC* (bottom) shown versus Clark Fork River at Missoula streamflow volume (1999–2015) with the correlation shown in scatterplot.

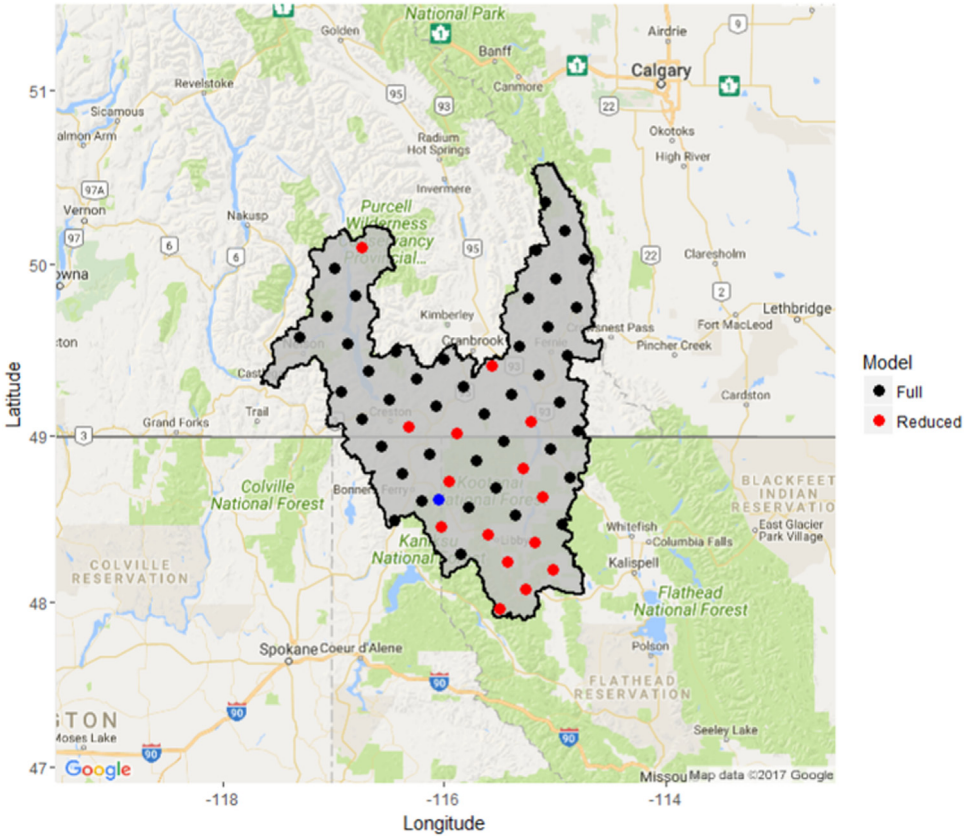

Fig. A12. IMS sample locations in the Kootenai subbasin for the Full *PSC* metric (left) as well as Reduced *PSC* metric (right).

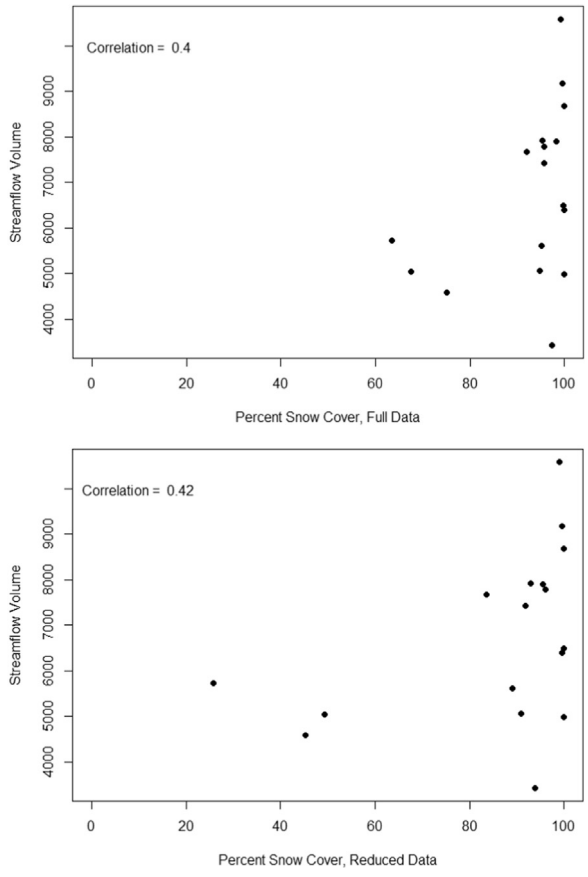

Fig. A13. Full *PSC* (top) and Reduced *PSC* (bottom) shown versus Kootenai River at Leonia streamflow volume (1999–2015) with the correlation shown in scatterplot.

References

Andreadis, K.M., Lettenmaier, D.P., 2006. Assimilating remotely sensed snow observations into a macroscale hydrology model. Adv. Water Resour. 29 (6), 972 (886).

Bergeron, J., Royer, A., Turcotte, R., Roy, A., 2014. Snow cover estimation using blended MODIS and AMSR-E data for improved watershed-scale spring streamflow simulation in Quebec, Canada. Hydrol. Process. 28, 4626–4639. http://dx.doi.org/10.1002/hyp.10123.

Biggs, T.W., Whitaker, T.M., 2012. Critical elevation zones of snowmelt during peak discharges in a mountain river basin. J. Hydrol. 438–439, 52–65. http://dx.doi.org/10.1016/j.jhydrol.2012.02.048.

Derksen, C., LeDrew, E., 2000. Variability and change in terrestrial snow cover: data acquisition and links to the atmosphere. Progress. Phys. Geogr. 24, 469–498.

Estilow, T.W., Young, A.H., Robinson, D.A., 2015. A long-term northern Hemisphere snow cover extent data record for climate studies and monitoring. Earth Syst. Sci. Data 7, 137–142. http://dx.doi.org/10.5194/essd-7-137-2015.

Gleason, K.E., Nolin, A.W., Roth, T.R., 2016. Developing a representative snow monitoring network in a forested mountain watershed. Hydrol. Earth Syst. Sci. Discuss. http://dx.doi.org/10.5194/hess-2016-317.

Hall, D.K., Foster, J.L., DiGirolamo, N.E., Riggs, G.A., 2012. Snow cover, snowmelt timing and stream power in the Wind River Range, Wyoming. Geomorphology 137 (2012), 87–93. http://dx.doi.org/10.1016/j.geomorph.2010.11.011.

Helfrich, S.R., McNamara, D., Ramsay, B.H., Baldwin, T., Kasheta, T., 2007. Enhancements to, and forthcoming developments in the Interactive multisensor snow and ice mapping system (IMS). Hydrol. Process. 21, 1576–1586. http://dx.doi.org/10.1002/hyp.6720.

Helfrich, S.R., Li, M., Kongoli, C., 2012. Interactive Multisensor Snow and Ice Mapping System Version 3 (IMS V3) Algorithm theoretical basis document version 2.0 Draft 4.1. NOAA NESDIS Center for Satellite Applications and Research (STAR), pp. 59.

Historical High Water Events, 2014. 〈http://orsolutions.org/wp-content/uploads/2014/10/Historic-High-Water-Portland-Fact-Sheet.pdf〉 (Accessed 5 July 2016).

Kumar, S., Peters-Lidard, C., Mocko, D., Tian, Y., 2013. Multiscale Evaluation of the improvements in surface snow simulation through terrain adjustments to radiation. J. Hydrometeor. 14, 220–232. http://dx.doi.org/10.1175/JHM-D-12-046.1.

Liu, Y., Peters-Lidard, C.D., Kumar, S.V., Arsenault, K.R., Mocko, D.M., 2015. Blending satellite-based snow depth products with in situ observations for streamflow predictions in the Upper Colorado River Basin. Water Resour. 51, 1182–1201. http://dx.doi.org/10.1002/2014WR016606.

McCabe, G.J., Clark, M.P., 2005. Trends and variability in snowmelt runoff in the western United States. J. Hydrometeor. 6, 476–482.

McGuire, M., Wood, A.W., Hamlet, A.F., Lettenmaier, D.P., 2006. Use of satellite data for streamflow and reservoir storage forecasts in the Snake River Basin. J. Water Resour. Plan. Manag. 132 (2), 97–110.

Molotch, N.P., Bales, R.C., 2006. SNOTEL representativeness in the Rio Grande headwaters on the basis of physiographics and remotely sensed snow cover persistence. Hydrol. Process. 20, 723–739. http://dx.doi.org/10.1002/hyp.6128.

Mote, P.W., 2003. Trends in snow water equivalent in the Pacific Northwest and their climatic causes. Geophys. Res. Lett. 30. http://dx.doi.org/10.1029/2003GL017258.

Nagler, T., Rott, H., Malcher, P., Müller, F., 2008. Assimilation of meteorological and remote sensing data for snowmelt runoff forecasting. Remote Sens. Environ. 112 (4), 1408–1420.

National Ice Center, 2008. Updated Daily. IMS Daily Northern Hemisphere Snow and Ice Analysis at 1-km, 4-km, and 24-km Resolutions, Version 1. 1999–2015. NSIDC: National Snow and Ice Data Center, Boulder, Colorado USA. http://dx.doi.org/10.7265/N52R3PMC. (Accessed 7 January 2016).

Nolin, A.W., Brown, A., 2008. Assessing the representativeness of the NRCS SNOTEL system at a basin-wide scale. In: Proceedings of the 76th Annual Western Snow Conference. April 2008, Hood River, OR.

O'Connor, J.E., Costa, J.E., 2000. Large floods in the United States: Where they happen and why. U. S. Geol. Surv. Circ. 1245, 19.

Parajka, J., Blöschl, G., 2008. Spatio-temporal combination of MODIS images–potential for snow cover mapping. Water Resour. Res. 44 (3).

Ramsay, B.H., 1998. The interactive multisensor snow and ice mapping system. Hydrol. Process. 12, 1537–1546. http://dx.doi.org/10.1002/(SICI)1099-1085(199808/09)12:10/11<1537::AID-HYP679>3.0.CO;2-A.

Rango, A., Salomonson, V., Foster, J., 1977. Seasonal streamflow estimation in the Himalayan region employing meteorological satellite snow cover observations. Water Resour. Res. 13, 109–112.

Rango, A., Martinec, J., 1979. Application of a snowmelt-runoff model using Landsat data. Nord. Hydrol. 10, 225–238.

Rango, A., 1993. Snow hydrology processes and remote sensing. Hydrol. Proc. 7, 121–138. http://dx.doi.org/10.1002/hyp.3360070204.

Robinson, D.A., Dewey, K.F., Heim Jr., R., 1993. Global snow cover monitoring: an update. Bull. Am. Meteorol. Soc. 74, 1689–1696. http://dx.doi.org/10.1175/1520-0477(1993)074%3C1689:GSCMAU%3E2.0.CO;2.

Serreze, M.C., Clark, M.P., Armstrong, R.L., 1999. Characteristics of the western United States snowpack from snowpack telemetry (SNOTEL) data. Water. Res. 35 (7), 2145–2160.

Tong, J., Dery, S.J., Jackson, P.L., Derksen, C., 2010. Snow distribution from SSM/I and its relationships to the hydroclimatology of the Mackenzie River Basin, Canada. Adv. Water Resour. 33 (6), 667–677 (2010).

U.S. Geological Survey, 2012. National Water Information System data available on the World Wide Web (USGS Water Data for theNation), (Accessed 15 October 2015), atURL 〈http://waterdata.usgs.gov/nwis/〉.

Wickham, H., 2009. ggplot2: Elegant Graphics for Data Analysis. Springer-Verlag, New York.

Yang, D., Robinson, D.A., Zhao, Y., Estilow, T., Ye, B., 2003. Streamflow response to seasonal snow cover extent changes in large Siberian watersheds. J. Geophys. Res. 108, 2156–2202. http://dx.doi.org/10.1029/202JD003149.

Yang, D., Zhao, Y., Armstrong, R., Robinson, D.A., 2009. Yukon River streamflow response to seasonal snow cover changes. Hydrol. Process. 23, 109–121. http://dx.doi.org/10.1002/hyp.7216.

Zhou, X., Xie, H., Hendrickx, J.M.H., 2005. Statistical evaluation of remotely sensed snow-cover products with constraints from streamflow and SNOTEL measurements. Remote Sens. Environ. 94, 214–231.